Effect of third-order dispersion on nonlinear magnetostatic spin waves in ferromagnetic films

A. D. Boardman
Photonics and Nonlinear Science Group, Joule Laboratory, Department of Physics, University of Salford, Salford M5 4WT, United Kingdom

S. A. Nikitov
Institute of Radioengineering and Electronics, Russian Academy of Sciences, Mokhovaya Street, 11, 103907, Moscow, Russia

N. A. Waby, R. Putman, and H. M. Mehta
Photonics and Nonlinear Science Group, Joule Laboratory, Department of Physics, University of Salford, Salford M5 4WT, United Kingdom

R. F. Wallis
Department of Physics and Institute for Surface and Interface Science, University of California, Irvine, California 92717
(Received 17 May 1996; revised manuscript received 11 July 1996)

The effect of high-order dispersion on nonlinear magnetostatic spin waves has been investigated, theoretically, for ferromagnetic films that have metal plates near both surfaces of the film. The conditions under which third-order dispersion has to be considered are thoroughly analyzed and some numerical calculations concerning the propagation of short microwave pulses in ferromagnetic films are presented. [S0163-1829(98)10717-8]

I. INTRODUCTION

Recent developments in the theory and observation of magnetostatic waves show that their nonlinear characteristics are both extremely interesting and of potential practical importance. The favored experimental system consists of a thin film of yttrium iron garnet (YIG) that is biased, in certain, well-defined, ways, by an external magnetic field. Although the insulator YIG is a classic example of a ferromagnetic material, it consists of 20 sublattices and the oscillations of these sublattices, relative to one another, are generated at frequencies greater than 10^3 GHz. At the lower (practical) frequencies (8–12 GHz), to be considered, here these sublattices move together so that YIG behaves, quite simply, as a ferromagnet, with a total saturated magnetic moment. For this reason, this investigation considers only the ferromagnetic state, even though data relevant to YIG are used. In a typical experiment, a YIG film is grown onto a nonmagnetic substrate and the magnetostatic waves are waves generated in its spin system through a thin metal microstrip transducer placed on the surface of the device perpendicular to the propagation direction.

The famous magnetostatic waves that have attracted a lot of attention down the years are called,[1,2] respectively, *forward volume*, *backward volume*, and *surface waves*. The intense investigation of the many linear properties of these waves is now being matched by investigations of these nonlinear properties and they are now attracting a lot of attention. They involve new areas that have generic properties, overlapping onto other disciplines of physics, like optics. Foremost among these is the evolution of solitonlike behavior of temporal input pulses as they progress down a magnetic film to a second, thin metal strip, receiving transducer.

Many waveguide structures are possible, but the one that is addressed here is shown in Fig. 1. It shows the introduction of metal plates that can be close to the surfaces[3–7] of a ferromagnetic film, but for the sake of clarity, the input/output transducers are omitted. The linear properties of this metal-ferromagnetic-metal structure were analyzed some time ago,[3–7] with the main outcome being that the metal can seriously modify the dispersion characteristics expected of a free-standing ferromagnetic film. This information is still required here because nonlinear theory demands both a knowledge of the *linear dispersion* of the magnetostatic wave, i.e., the variation of angular frequency ω with the wave number, k, and a knowledge of the *nonlinear power shift* of band edges. It is important,[8] therefore, to acquire a knowledge of the *linear* dispersion derivatives $\partial\omega/\partial k$, $\partial^2\omega/\partial k^2$, and $\partial^3\omega/\partial k^3$, evaluated at some operating frequency $\omega=\omega_0$. An initial point is that it is interesting to discover that the presence of metal plates can force $\omega''=\partial^2\omega/\partial k^2$ to be zero, at some wave numbers. To discuss this feature, definitions used

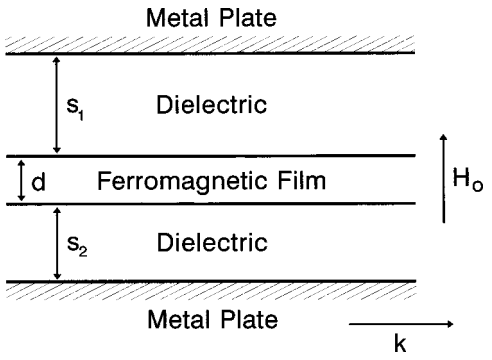

FIG. 1. Sketch of a ferromagnetic film, of thickness d, with a metal plate a distance s_1 away from the top surface and a metal plate distance s_2 away from the bottom surface. The external magnetic field H_0 is perpendicular to the film so that the film is in the forward volume magnetostatic wave configuration.

in the optics literature can be usefully introduced. First note that $\partial^2 k/\partial\omega^2 = -(1/|v_g|^3)\partial^2\omega/\partial k^2$, where $v_g = \partial\omega/\partial k$ is the group velocity, and then call $\partial^2 k/\partial\omega^2$ the *group-velocity dispersion* (GVD).[8] In this language, it can be said that the metal plates can cause GVD to vanish at a certain wave number.[7] Indeed, the main feature appearing in the dispersion curve (i.e., the spectrum or ω vs k) is an inflection point, where the second-order dispersion $\partial^2\omega/\partial k^2$ goes to zero, so that the propagation of nonlinear magnetostatic pulses, centered upon such a point, will be controlled by third-order dispersion $\partial^3\omega/\partial k^3$, as will be demonstrated below.

II. BASIC CONCEPTS

Suppose that the nonlinear dispersion equation for magnetostatic waves, propagating in a ferromagnetic film, is written formally as[9]

$$[\omega - \omega(k,|\phi|^2)]\phi = 0, \tag{1}$$

where ϕ is the amplitude of the wave. This relationship contains the dependence of the angular frequency ω upon the external magnetic field, and information about the geometrical configuration of the waveguide. A magnetostatic envelope pulse is really a *fast* carrier wave, such as $\exp i(k_0 x - \omega_0 t)$, modulated by a *slowly* varying pulse amplitude $\phi(x,t)$, where t is time and x is selected as the propagation direction. A Taylor expansion of Eq. (1), around an operating point (ω_0, k_0), yields the expression[9,10]

$$\left[\omega - \omega_0 - \left(\frac{\partial\omega}{\partial k}\right)_{k_0}\kappa_x - \frac{1}{2}\left(\frac{\partial^2\omega}{\partial k^2}\right)_{k_0}\kappa_x^2 - \frac{1}{6}\left(\frac{\partial^3\omega}{\partial k^3}\right)_{k_0}\kappa_x^3 - \left(\frac{\partial\omega}{\partial|\phi|^2}\right)_0 |\phi|^2\right]\phi = 0, \tag{2}$$

where dispersion *and* a nonlinear frequency shift $(\partial\omega/\partial|\phi|^2)_0|\phi|^2$ are incorporated. Specifically, a small deviation, due to dispersion, drives the wave number $\mathbf{k}_0 = (k_0,0,0)$ to $\mathbf{k} = \boldsymbol{\kappa} + \mathbf{k}_0$, where $\boldsymbol{\kappa} = (\kappa_x,0,0)$ and $\kappa_x \ll k_0$. Making a transformation to the operator language $(\omega - \omega_0) = i(\partial/\partial t)$ and $\kappa_x = -i(\partial/\partial x)$ gives

$$i\frac{\partial\phi}{\partial t} + i\left(\frac{\partial\omega}{\partial k}\right)_{k_0}\frac{\partial\phi}{\partial x} + \frac{1}{2}\left(\frac{\partial^2\omega}{\partial k^2}\right)_{k_0}\frac{\partial^2\phi}{\partial x^2} - \frac{i}{6}\left(\frac{\partial^3\omega}{\partial k^3}\right)_{k_0}\frac{\partial^3\phi}{\partial x^3} - \gamma|\phi|^2\phi = 0, \tag{3}$$

where $\gamma = (\partial\omega/\partial|\phi|^2)_0$ is to be called the nonlinear coefficient.[9,11–13] Equation (3) can be recast, selecting a frame of reference moving with a group velocity $v_g = (\partial\omega/\partial k)_{k_0}$, by the transformations[8,12,13] $T = t$, $X = x - v_g t$, which imply that

$$\frac{\partial}{\partial t} = \frac{\partial X}{\partial t}\frac{\partial}{X} + \frac{\partial T}{\partial t}\frac{\partial}{\partial T} = -v_g\frac{\partial}{\partial X} + \frac{\partial}{\partial T};$$

$$\frac{\partial}{\partial x} = \frac{\partial X}{\partial x}\frac{\partial}{\partial X} + \frac{\partial T}{\partial X}\frac{\partial}{\partial T} = \frac{\partial}{\partial T}. \tag{4}$$

Hence, Eq. (3) becomes

$$i\frac{\partial\phi}{\partial T} + \mathrm{sgn}(\omega'')\frac{|\omega''|}{2}\frac{\partial^2\phi}{\partial X^2} - \frac{i}{6}\mathrm{sgn}(\omega''')|\omega'''|\frac{\partial^3\phi}{\partial X^3} - \mathrm{sgn}(\gamma)|\gamma||\phi|^2\phi = 0, \tag{5}$$

where $\omega'' = (\partial^2\omega/\partial k^2)_{k_0}$ and $\omega''' = (\partial^3\omega/\partial k^3)_{k_0}$. This equation also shows that the characteristic times[8,12–16] $t_D^{(2)} = D_0^2/|\omega''|$, $t_D^{(3)} = D_0^3/|\omega'''|$ can be, profitably, introduced, where D_0 is the spatial pulse length along the x axis of propagation. In addition, if it is desirable, the relationships $k'' = \partial^2 k/\partial\omega^2 = -1/v_g^3\omega''$, $k''' = -1/v_g^4\omega'''$, $D_0 = v_g T_0$ can be used, where T_0 is the temporal length of the pulse. When this is the case, the dispersion of a pulse operates over the length scales[8]

$$L_D^{(2)} = \frac{T_0^2}{|k''|}, \quad L_D^{(3)} = \frac{T_0^3}{|k'''|}. \tag{6}$$

Choosing to measure T in units of $t_D^{(2)}$, and X in units of D_0, leads to

$$i\frac{\partial\phi}{\partial\tau} + \frac{1}{2}\mathrm{sgn}(\omega'')\frac{\partial^2\phi}{\partial\xi^2} - \frac{i}{6}\mathrm{sgn}(\omega''')\frac{t_D^{(2)}}{t_D^{(3)}}\frac{\partial^3\phi}{\partial\xi^3} - t_D^{(2)}\mathrm{sgn}(\gamma)|\gamma||\phi|^2\phi = 0. \tag{7}$$

The ratio $t_D^{(2)}/t_D^{(3)} = |\omega'''|/[|\omega''|v_g T_0] = |k'''|/T_0|k''|$ can be used[8] to determine whether third-order dispersion is important, provided that $|k''| \neq 0$.

A comment on the use of Taylor's theorem, in the derivation of the nonlinear Schrödinger equation, is appropriate at this point. For a dispersion equation that is *precisely* a polynomial of nth degree, the coefficients of this polynomial are exactly the derivatives of ω (with respect to k), evaluated at k_0. If the dispersion equation is actually like this, then the magnitudes of the coefficients will be dictated by the properties of the equation and they can be large, or small, or *identically* zero. If Taylor's theorem for an arbitrary function (a complicated dispersion equation) is used, then this function is not necessarily a polynomial and the resulting formula can lead only to an *approximation* to the function by a polynomial. The dispersion equation must possess continuous derivatives up to $(n+1)$th order, and then there will be a *remainder*. That this remainder must be negligible is obvious, if a fair representation of the dispersion equation, in the neighborhood of the operating point, is to be relied upon. In the optics literature, Eq. (3) has actually been used when $\omega'' = 0$, thus forcing a consideration of $\omega''' \neq 0$. It has also been used when $\omega'' \neq 0$, $\omega''' \neq 0$, thus forcing a comparison of the two terms contributing the dispersion.[8] In the latter case, the consistent approach is to demand convergence, in the sense that the third-order dispersion term is *less* than the second-order dispersion term. If this is the consideration, then *both* $|\omega'''| \neq 0$ *and* $|\omega''| \neq 0$, and third-order dispersion is only significant when the pulse length T_0 satisfies the inequality $T_0 < |\omega'''|/(|\omega''|v_g)$. This inequality need not be applied because it is the special case,[8] $|\omega''| = 0$, that is presented here. The aim is to show, for the magnetic case, how pulses evolve when only third-order dispersion is operative.

For a *linear* film with $|\omega''| = 0$, a given input pulse evolves with oscillations that plunge to zero at their minima,

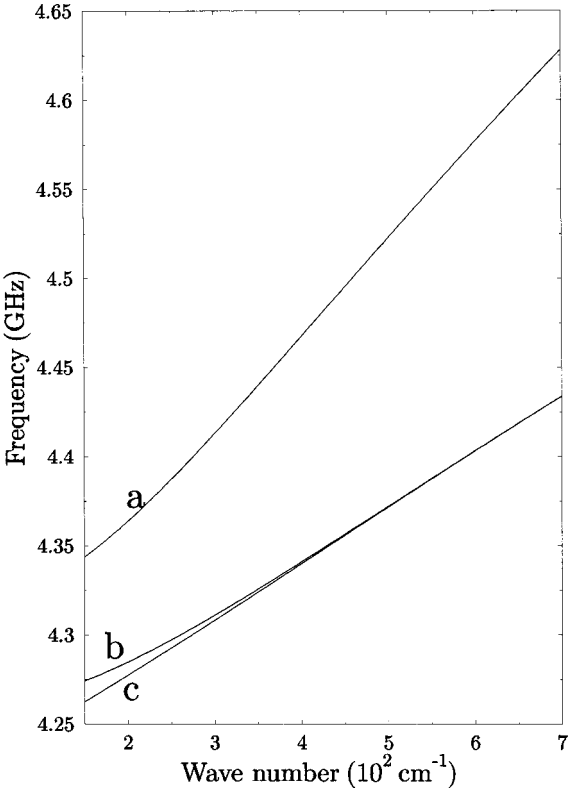

FIG. 2. Dispersion curves for forward volume magnetostatic waves. The ferromagnetic film thickness is $d=3$ μm and the internal magnetic field is $H_0-4\pi M_0=1500$ Oe. The saturation magnetization is $4\pi M_0=1750$. The top metal plate is fixed at a distance of $s_1=60$ μm. The bottom metal plate is positioned at (a) 0 μm, (b) 60 μm, and (c) ∞ μm.

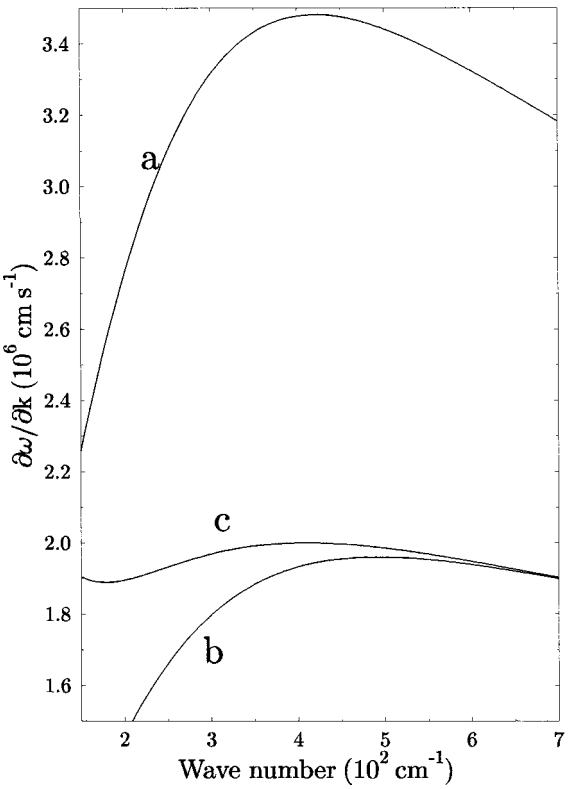

FIG. 3. Group velocity vs wave number for the dispersion curves displayed in Fig. 2.

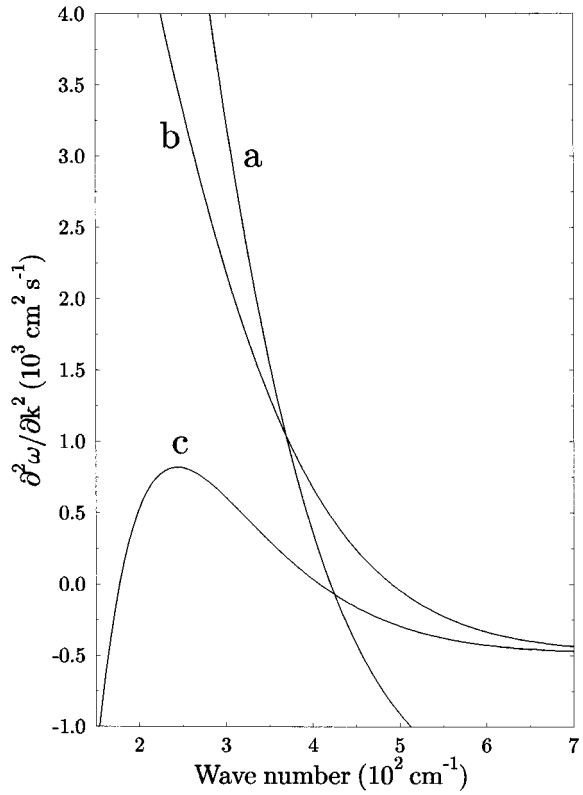

FIG. 4. Second-order dispersion vs wave number for the dispersion curves of Fig. 2.

near to the trailing or leading edges of the pulse. For a *nonlinear* film, self-phase modulation will increase the number of these oscillations[8] and also raise the minima from zero. The reason for this is that the nonlinearity permits the pulse to develop an *effective* $|\omega''|=\omega'''|\delta\omega|/(2\pi v_g)$, where[8,17] $\delta\omega=\Gamma/T_0\delta$ is the *maximum chirp*, created by self-phase modulation, T_0 is the pulse width, Γ is a dimensionless constant, and δ is the self-phase modulation-induced phase shift. The constant Γ depends upon the shape of the input pulse. While it is not appropriate here to list Γ values for a whole variety of input pulses, it can easily be shown, for a Gaussian input pulse,[8] that $\Gamma=\sqrt{2}e^{-0.5}=0.86$. This is simply obtained by calculating the self-phase modulation-induced chirp $\delta\omega$ for an input pulse of the form $\exp[-T^2/(2T_0^2)]$, where T is the local time measured across the pulse. The maximum self-phase modulation phase shift occurs at the pulse center[8] and, in this formulation, is given by $\delta=\gamma|\phi|^2t$, where t is the elapsed time since the input occurred and γ is the nonlinear coefficient introduced in Eq. (3). For typical data,[12–16] $|\omega''|\simeq 10^3-10^4$ cm^2 s^{-1}, which shows that sufficient chirp is created by the self-phase modulation, at this pulse length, to influence the pulse evolution in magnetic film. Clearly, the pulse length matters and the induced dispersion will become dominant as T_0 gets smaller. Furthermore, if the pulse propagates far enough, a soliton will be created,[17] because, spectrally, the pulse energy concentrates into the anomalous, or normal, dispersion frequency regions. In other words, the oscillations that appear in the evolving pulse eventually disperse, and a stable soliton appears. For a given system, however, the soliton period may be longer than the device, so only the nonlinear, nonstationary state evolution will be observed.

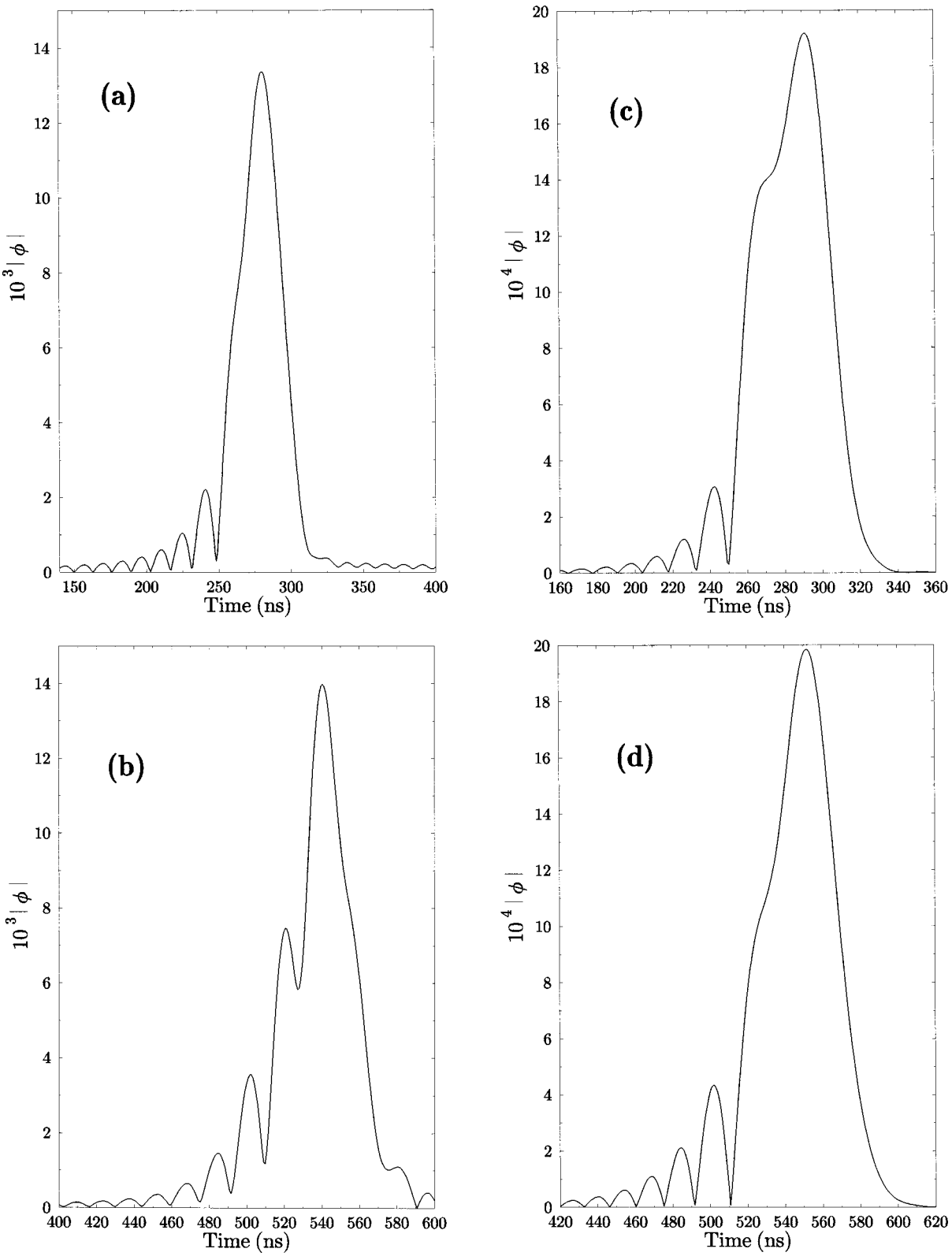

FIG. 5. Evolution of a nonlinear forward volume magnetostatic wave rectangular input pulse. The pulse propagates at a zero GVD point, at which $k_0 = 179\ \text{cm}^{-1}$, $\omega/2\pi = 4.272$ GHz, $(\partial\omega/\partial k)_{k_0} = 1.89\times10^6\ \text{cm s}^{-1}$, $(\partial^3\omega/\partial k^3)_{k_0} = 29.8\ \text{cm}^3\ \text{s}^{-1}$ and $\gamma = 3.08\times10^{10}\ \text{rad s}^{-1}$. Curves (a) and (b) show the development of a 40 ns, $N=5$, $|\phi_0| = 7.48\times10^{-3}$ input pulse as it reaches $x = 0.5$ cm and $x = 1.0$ cm, respectively. Curves (c) and (d) show a 50 ns, $N=1$, $|\phi_0| = 1.07\times10^{-3}$ input pulse as it reaches $x = 0.5$ cm and $x = 1.0$ cm, respectively. Curve (e) shows how a 100 ns $N=2$, $|\phi_0| = 7.57\times10^{-4}$ input pulse has developed at $x = 0.5$ cm, while curve (f) shows how a 100 ns $N=1$, $|\phi_0| = 3.79\times10^{-4}$ input pulse has evolved at $x = 1.0$ cm.

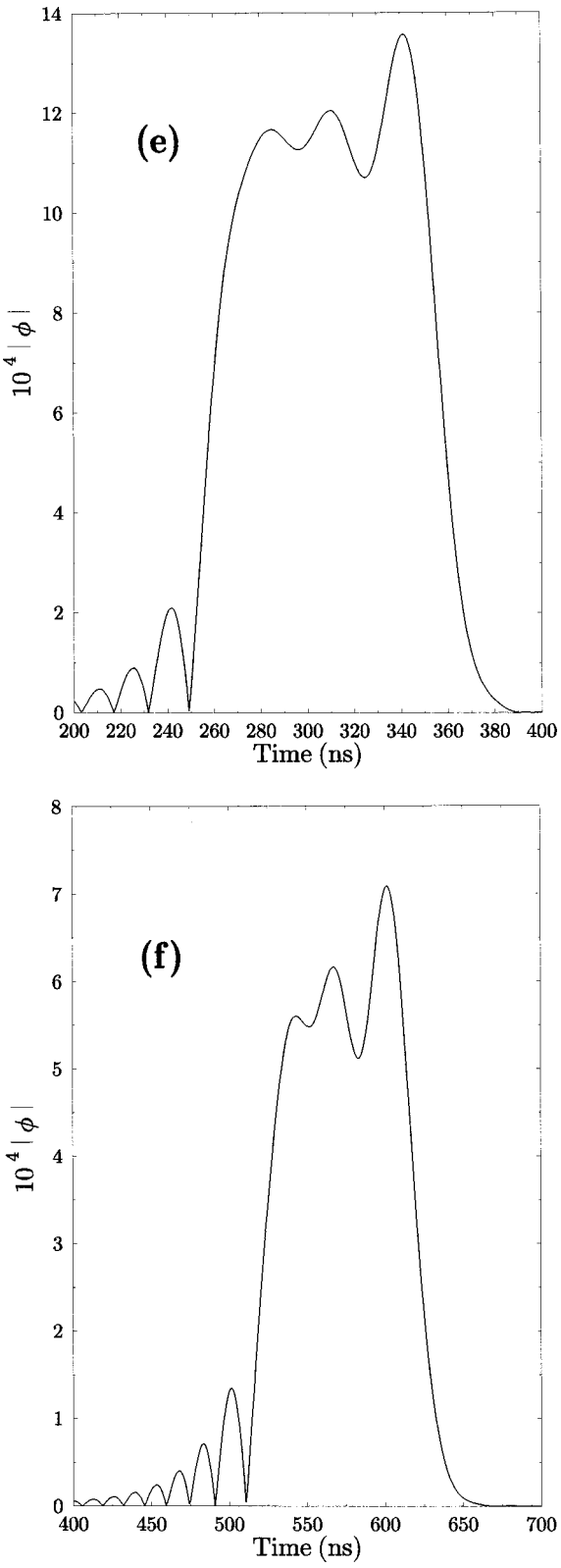

FIG. 5. (*Continued.*)

III. NUMERICAL ANALYSIS AND DISCUSSION

Figure 2 shows some typical curves for a ferromagnetic film of thickness $d=3\ \mu$m, with $s_1=60\ \mu$m and s_2 taking on the values 0 μm (curve *a*), 60 μm (curve *b*), and ∞ μm (curve *c*). Only the forward volume magnetostatic wave is discussed here and it propagates with wave number k in the plane of the ferromagnetic film but perpendicular to the applied field H_0. In this problem, then, the *internal field* is $H_0-4\pi M_0=1500$ Oe, where $4\pi M_0=1750$ Oe is the saturation magnetization. The linear curves have been generated afresh here, but the general topic can be checked in the literature, where it is the ferromagnetic behavior of YIG films that is used. Figures 3 and 4 contain plots of the variation of the group velocity $\partial\omega/\partial k$ and the second derivative $\partial^2\omega/\partial k^2$, which is simply related to the GVD. The main point of this discussion is that the GVD *vanishes* at certain points.

Figure 5 shows what happens as a rectangular input pulse length is varied for the metal plate-backed waveguide of Fig. 1, $s_1=60\ \mu$m, $s_2=\infty\ \mu$m. The input power is also varied by choosing the value of $N^2=L_D^{(3)}/L_{NL}$, where $L_{NL}=|v_g|/\gamma|\phi_0|^2$ and $|\phi_0|$ is the peak amplitude of the input magnetostatic pulse. The operating frequency is $\omega/2\pi=4.262$ GHz, the zero GVD point is $k_0=179\ \mathrm{cm}^{-1}$ and the forward volume magnetostatic wave is the selected configuration. The group velocity, at $k=k_0$, is $(\partial\omega/\partial k)_{k_0}=1.89\times10^6\ \mathrm{cm\ s}^{-1}$, $\gamma=3.08\times10^{10}\ \mathrm{rad\ s}^{-1}$ and $(\partial^3\omega/\partial k^3)_{k_0}=29.8\ \mathrm{cm}^3\ \mathrm{s}^{-1}$ and the series $\omega=\omega_0+\omega'\kappa_x+\omega'''\kappa_x^3+\ldots$ is set to converge for this data set, given that $\kappa_x=2\pi(T_0v_g)^{-1}$, where T_0 is the temporal pulse length. From the optics literature[8,17] the *numerical* rule of thumb is that a sechlike pulse evolves to a first-order (fundamental) soliton over a distance $x=10T_0^3/(|k'''|N^2)$, which for the model being used here is $x=10T_0^3v_g^4/[|\omega'''|N^2]$. It is of considerable interest to know if this length is longer than, or less than, the typical length between the input and receiving microstrips of the magnetostatic waveguide being investigated here. Even if evolution to a soliton does not occur, the nonlinear development must be determined as a function of input pulse width. The rule stated above is based upon a hyperbolic secant input so it will not apply, precisely, to the rectangular input pulse. It is, nevertheless, a reasonable guide because we do not wish to know *precisely* the soliton period. A good estimate will be a sufficient driver for a device design.

There is another interesting feature of the simulations to be discussed below and that is introduced by the boundary conditions. In simulations based upon Eq. (3), the input pulse must be started up on the t axis or the x axis. Conventionally, the initial condition is set upon the x axis.[18] Such a condition presents problems of physical interpretation in *real units*, however. In practice, a pulse is ''switched on,'' allowing the pulse to be of a certain duration, so using the time axis makes physical sense. Accordingly, all the simulations presented here have been generated from this type of initial condition. Specifically, the nonlinear Schrödinger equation has been solved in the laboratory frame and the method of solving it is called forcing.[19] The work of Kaup and Hanson is very interesting because it raises the problem of how to *count* the number of solitons expected from a given output pulse. Inverse scattering theory will yield exact conclusions for the conventional input on the x axis but this method is likely to fail[19] if the time axis is used by ''switching on'' the initial pulse for a certain period of time. In fact, Kaup and Hanson have put forward an empirical approach to soliton counting but this is not the main concern here. The principal point of interest is to establish a set of results that show at

least part of the relationships between pulse length, third-order dispersion, and induced-second-order dispersion. In this case, in which third-order dispersion is capable of producing pulse asymmetry, accompanied by quite strong oscillations, it remains to be seen whether ''forcing'' can impose its own asymmetry on the pulse.[12–15]

Figure 5 shows a sequence of simulations for $|\omega''|=0$ in which the input temporal pulse length and/or the input power is varied. In the simulations to be reported below it is accepted[17] that the initial pulse will evolve into a stationary state (a first-order soliton) and dispersed energy. The simulations could have been allowed to progress until this occurred but the propagation distances would have exceeded possible device lengths. For this type of magnetic system the output is characteristic of the earlier nonstationary part of the evolution process. The main points to look for in the results are (1) as T_0 gets larger, the forced boundary conditions will be more apparent, and (2) as N gets larger, coupled to T_0 getting smaller, the possibility of soliton formation, within the device length is significantly greater. Given these guidelines, Fig. 5 can be discussed in a semiquantitative way. Figures 5(a) and 5(b) show what happens to a 40 ns, $N=5$, rectangular input pulse by the time the propagation distance has reached $x=0.5$ cm and $x=1$ cm, respectively. The question of whether ''forcing'' has any impact on the pulse shape will be addressed first. A magnetic system is highly dispersive and typical group velocities are several orders of magnitude less than the velocity of light. This means that magnetic systems are rather different, in their pulse response behavior, from optical fibers. If a, temporally, long pulse is entered into a magnetostatic wave system, it begins to disperse strongly as soon as it is being entered. This means that under ''forced'' boundary conditions $|\omega''|\neq 0$ dispersion will result in an early asymmetric development.[12–16] Figures 5(a) and 5(b) do show an asymmetry, but it is due, in this case, to the $|\omega'''|$ dispersion, which gives rise to oscillations on the leading edge (because $\omega'''>0$) of the pulse. Because $N=5$, the input power is quite high, however, so self-phase modulation is also significant early on in the pulse development. The existence of self-phase modulation lifts the minima, of Fig. 5(a), above zero and the pulse sees an *effective* ω'' that will lead, ultimately, to soliton formation plus the radiation of the energy associated with the ''unwanted'' oscillations. For this case, a fundamental soliton will not appear until $x \sim 10.87$ cm. In view of the loss that there would be in a real system, this is too great a propagation distance to permit experimental observation of a soliton in a magnetic film.

Figures 5(c) and 5(d) show the state of a lower power ($N=1$), broader, rectangular input pulse ($T_0=50$ ns) at $x=0.5$ cm and $x=1.0$ cm, respectively. Already it can be seen that there is now not enough self-phase modulation to lift the minima from zero and that soliton formation, by the time $x=1.0$ cm is reached, is not even close. In fact, for this case, a soliton will not appear until $x=106$ cm, which demonstrates how critical T_0 and N are to the chances of soliton formation. In the results shown in Figs. 5(c) and 5(d), apart from the oscillations expected from the role of $|\omega'''|$, asymmetry is beginning to appear in the main part of the pulse, because of the ''forced'' way in which the pulse is entered into the system.[19]

The final pair of simulations are shown in Figs. 5(e) and 5(f), which are for pulse lengths of 100 ns and for $N=2$ and $N=1$, respectively. For these cases, the distances at which a fundamental soliton will form are the order of a km, so such a formation is out of the question, in practice. Oscillations due to $|\omega'''|$ appear, as expected, on the leading edge of the pulse, but there is significant distortion from the boundary conditions. In other words, a pulse length of 100 ns is very long, for this system, and significant dispersion is taking place as the pulse is being entered into the waveguide.

IV. CONCLUSIONS

The aim of this paper is to study the power dependence of a magnetic system, which is, at the linear (low power) level, controlled by third-order dispersion. As is usually the case, the interest centers upon the differences, or equalities, to dispersive optical systems. For the latter there is already information[8,17] on the role of third-order dispersion. The differences in (by several orders of magnitude) the group velocities associated with optical or magnetic systems, however, has meant that the magnetics cases are especially interesting.[12,13,15] For second-order dispersion, early asymmetric pulse shape development and using the *forced nonlinear Schrödinger* equation[19] is a lively topic of debate. Here we investigate third-order dispersion coupled to nonlinearity, produced by inputting rectangular pulses into a magnetic thin film controlled by a metal plate. The simulations are produced, therefore, on a scale of nanoseconds and the principal interest lies in the extent to which the generically accepted[8,17] properties of nonlinear-third-order coupling is all that can appear for this magnetic system. If not, do the boundary conditions, i.e., using the forced nonlinear Schrödinger equation,[19] become dominant, thus permitting the magnetic character of the system to emerge? The conclusion reached here is that the pulse width, in time, controls the outcome. For relatively small pulse lengths (40 ns), third-order dispersion dominates in the early part ($x=0.5$ cm) of the pulse development (with the expected set of subsidiary peaks[8,17]) but gives way to induced-second-order dispersive effects at a longer propagation distance ($x=10$ cm). For longer pulse lengths (50 ns and 100 ns) the boundary conditions become important and the now classic asymmetry[12,13,15] in the evolution of the main peak appears quite strongly. This is now very different from the optical case. Hence, for high input powers and small pulse widths, the magnetic case has evolution features similar to the optical case; but for lower input powers and longer pulses, asymmetric development, directly related to the much lower magnetic group velocity, appears. Metal plate controlled magnetic thin film designs need to take this into account.

ACKNOWLEDGMENTS

S.A.N. is gratefully indebted to the Alexander von Humboldt Foundation for partial financial support during this work. The authors A.D.B. and R.F.W. were supported in part by the NSF Grant Nos. DMR-9319404 and INT9224574. N.A.W. acknowledges support from the UK Engineering and Physical Research Council (EPSRC).

[1] R. W. Damon and J. R. Eshbach, J. Phys. Chem. Solids **19**, 308 (1961).
[2] A. D. Boardman, Yu. V. Gulyaev, S. A. Nikitov, and W. Qi, *Nonlinear Waves in Solid State Physics*, edited by A. D. Boardman, M. Bertolotti, and T. Twardowski (Plenum, New York, 1990).
[3] W. L. Bongianni, J. Appl. Phys. **43**, 2541 (1972).
[4] T. Yukawa, J. Yamada, K. Abe, and J. Ikenoue, Jpn. J. Appl. Phys. **16**, 2187 (1977).
[5] T. Yukawa, J. Ikenoue, J. Yamada, and K. Abe, J. Appl. Phys. **49**, 376 (1978).
[6] R. Marcelli and P. De Gasperis, IEEE Trans. Magn. **MAG-30**, 26 (1994).
[7] A. D. Boardman and S. A. Nikitov, Fiz. Tverd. Tela **31**, 1070 (1989) [Sov. Phys. Solid State **31**, 1070 (1989)].
[8] G. P. Agrawal, *Nonlinear Fiber Optics* (Academic, San Diego, 1989).
[9] A. K. Zvezdin and A. F. Popkov, Zh. Eksp. Teor. Fiz. **84**, 606 (1983) [Sov. Phys. JETP **57**, 350 (1983)].
[10] V. I. Karpman, *Nonlinear Waves in Dispersive Media* (Pergamon, Oxford, 1985).
[11] A. D. Boardman, Q. Wang, S. A. Nikitov, J. Shen, W. Chen, D. Mills, and J. S. Bao, IEEE Trans. Magn. **MAG-30**, 14 (1994).
[12] M. Chen, J. M. Nash, and C. E. Patton, J. Appl. Phys. **73**, 3906 (1993).
[13] A. D. Boardman, S. A. Nikitov, N. Xie, and H. Mehta, J. Magn. Magn. Mater. **145**, 357 (1995).
[14] M. Chen, M. A. Tsankov, J. M. Nash, and C. E. Patton, Phys. Rev. B **49**, 12 773 (1994).
[15] A. N. Slavin and G. M. Dudko, J. Magn. Magn. Mater. **86**, 115 (1990).
[16] M. Chen, M. A. Tsankov, J. M. Nash, and C. E. Patton, Phys. Rev. Lett. **70**, 1707 (1993).
[17] P. K. A. Wai, C. R. Menyuk, H. H. Chen, and Y. C. Lee, Opt. Lett. **12**, 628 (1987).
[18] J. Satsuma and N. Yajima, Prog. Theor. Phys. Suppl. **55**, 284 (1974).
[19] D. J. Kaup and P. J. Hanson, Physica D **18D**, 77 (1986).